ARMA 15-786

Hydraulic Fracturing in Shale with H_2O, CO_2 and N_2

Xiang Li[1]

[1]*John and Willie Leone Family Department of Energy and Mineral Engineering, EMS Energy Institute and G³ Center, The Pennsylvania State University, University Park, PA 16802, USA*

Zijun Feng[2] and Gang Han[3]

[2]*Department of Mining Engineering, Taiyuan University of Technology, Taiyuan, Shanxi 030024, China*

[3]*Aramco Services Company, Houston, TX 77096, USA*

Derek Elsworth[1,4] Chris Marone[4] Demian Saffer[4]

[4] *Department of Geosciences, EMS Energy Institute and G³ Center, The Pennsylvania State University, University Park, PA 16802, USA*

This paper was prepared for presentation at the 49th US Rock Mechanics / Geomechanics Symposium held in San Francisco, CA, USA, 28 June-1 July 2015.

This paper was selected for presentation at the symposium by an ARMA Technical Program Committee based on a technical and critical review of the paper by a minimum of two technical reviewers. The material, as presented, does not necessarily reflect any position of ARMA, its officers, or members. Electronic reproduction, distribution, or storage of any part of this paper for commercial purposes without the written consent of ARMA

ABSTRACT: Slick-water fracturing is the most routine form of well stimulation in shales; however N_2, LPG and CO_2 have all been used as "exotic" stimulants in various hydrocarbon reservoirs. We explore the use of these gases as stimulants on Green River shale to compare the form and behavior of fractures in shale driven by different gas compositions and states and indexed by breakdown pressure and the resulting morphology of the fracture networks. Fracturing is completed on cylindrical samples containing a single blind axial borehole under simple triaxial conditions with confining pressure ranging from 10~25MPa and axial stress ranging from 0-35MPa ($\sigma_1 > \sigma_2 = \sigma_3$). Results show that: 1) under the same stress conditions, CO_2 returns the highest breakdown pressure, followed by N_2, and with H_2O exhibiting the lowest breakdown pressure; 2) CO_2 fracturing, compared to other fracturing fluids, creates nominally the most complex fracturing patterns as well as the coarsest fracture surface and with the greatest apparent local damage; 3) under conditions of constant injection rate, the CO_2 pressure build-up record exhibits condensation between ~5-7MPa and transits from gas to liquid through a mixed-phase region rather than directly to liquid as for H_2O and N_2 which do not; 4) there is a positive correlation between minimum principal stress and breakdown pressure for failure both by transverse fracturing ($_3$ *axial*) and by longitudinal fracturing ($_3$ *radial*) for each fracturing fluid with CO_2 having the highest correlation coefficient/slope and lowest for H_2O. We explain these results in terms of a mechanistic understanding of breakdown, and through correlations with the specific properties of the stimulating fluids.

1 INTRODUCTION

Hydraulic fracturing is a mature completion technique which has been extensively applied in tight and unconventional gas reservoirs. For unconventional reservoirs such as shale with extremely low permeability, long horizontal laterals with multi-staged hydraulic fractures are necessary to deliver economic production. The introduction of hydraulic fractures significantly increases flow rate because of large surface contact area between fractures and the reservoir, enhanced permeability around the wellbore, and reduced fluid diffusion lengths (King, 2010; Vincent , 2010; Faraj & Brown, 2010).

Water-based fluids have become the predominant type of fracturing fluid. Sometimes N_2 or CO_2 gas is combined with the fracturing fluids to form foam as the base fluid. Other additives can also be combined with N_2 or CO_2 to improve the efficiency, eg. coupling solids-free viscoelastic surfactants (VES) with a carbon dioxide (CO2)-emulsified system to further enhance cleanup in a depleted reservoir, extend the application to water-sensitive formations, and maintain reservoir gas saturation to prevent any potential water blockage (Hall, et al., 2005); or incorporating low-polymer-loading carboxymethyl guar polymer and a zirconium-based crosslinker to minimize the damage and maximize production (Gupta, et al., 2009). For unconventional reservoirs in arid areas the availability of water is sparse. In these cases, N_2, liquefied petroleum gas (LPG) or CO_2 may become an "exotic" option for stimulation fluid. For example, fracturing with CO_2 has been used in places such as Wyoming where carbon dioxide supply and infrastructure are available (Bullis, 2013).

Using CO_2 or N_2 as stimulation fluid has a number

of potential advantages. Not only can it eliminate the need for large volume of water – approximately 5 million gallons per treatment – but it can also reduce the amount of wastewater produced and therefore reduce the environmental footprint of these operations. Energized fluids with a gas component can facilitate gas flowback in tight, depleted or water sensitive formations and may be required when drawdown pressures are smaller than the capillary forces in the formation (Friehauf & Sharma, 2009; Friehauf, 2009). Some recent studies suggest that using carbon dioxide can also result in a more extensive and interconnected network of fractures, making it easier to extract the resource (Ishida, et al., 2012; Alpern et al., 2013; Gan et al., 2013).

Classic geomechanics models suggest that breakdown pressure is independent of fluid type (composition) or state (gas or liquid) in that failure is controlled by effective stress, alone for a given rock tensile strength (Hubbert & Willis, 1957; Biot, 1941; Haimson & Fairhurst, 1967). However recent research suggests that fluid composition and/or state may have great influence on breakdown pressure (Alpern, et al., 2012; Gan, et al., 2013). This study explores the development and behavior of fractures in Green River shale when injected with H_2O, CO_2 and N_2 – with respect to breakdown pressures and the morphology of the resulting fracture network.

2 EXPERIMENTAL METHOD

The introduction and behavior of induced fractures in shale by H_2O, CO_2 and N_2 are investigated with respect to breakdown pressures and morphology of the resulting fracture networks. These experiments are conducted on Green River shale.

2.1 Approach

Hydraulic fracturing experiments are conducted using intact cylindrical cores containing a blind central borehole (~1/10-inch-diameter to depth of 1-inch). These experiments measure breakdown pressure and examine the morphology of the resulting fracture. Cores are 1-inch diameter and 2-inches long, sheathed in a jacket, and subjected to mean and deviatoric stresses in a simple triaxial configuration. Multiple cores of Green River shale are tested with H_2O, CO_2 and N_2.

2.2 Apparatus

All experiments in this study are completed using a standard triaxial apparatus configured for hydraulic fracturing as shown in Figs. 1 & 2. The triaxial core holder (Temco) accommodates the membrane-sheathed cylindrical samples (1-inch diameter and 2-inches long) and applies independent loading in the radial and axial directions *via* syringe pumps.

Fig. 1: Hydraulic fracturing system. Containment vessel with platen and fluid feed assembly and cell end-caps in foreground.

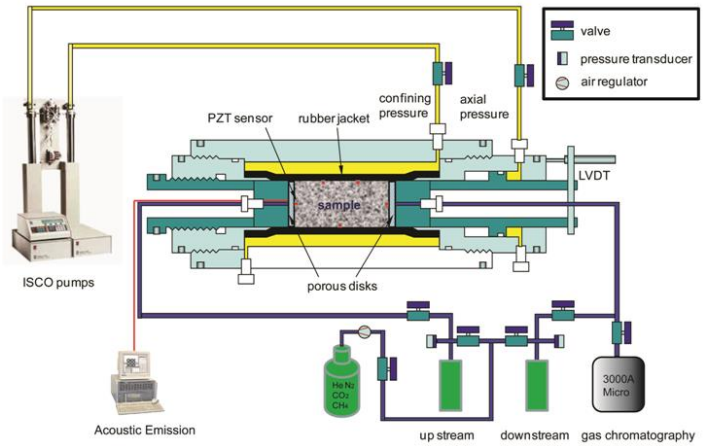

Fig. 2: Schematic of pulse test transient/hydraulic fracturing system (Wang, et al., 2011).

2.3 Sample Design and Seal Method

The samples are prepared as 1-inch diameter and 2-inch long cylindrical plugs with a blind borehole drilled axially to the sample mid-point (Fig. 3). Calibration experiments are conducted with 27 samples of Green River shale to explore the effectiveness of the method of sealing the sample, especially with corrosive and low viscosity CO_2. Calibration experiments are performed with three methods of sealing (Fig. 4) to ensure congruent results – with the simplest and least invasive of the methods used for the experimental suite. The

sealing methods are: (i) a platen with a single concentric O-ring encircling the central injection port (Fig 3(b)) (ii) a double O-ring design (Fig 3(c)); and (iii) use of a Swagelok fitting epoxied into the top borehole within the sample (Fig 3(d)). Of these, the double O-ring design is the preferred method – simple and adequate. The single O-ring is an effective seal for H_2O but not for CO_2. The fitting is an effective but unnecessary seal compared to the dual O-ring design.

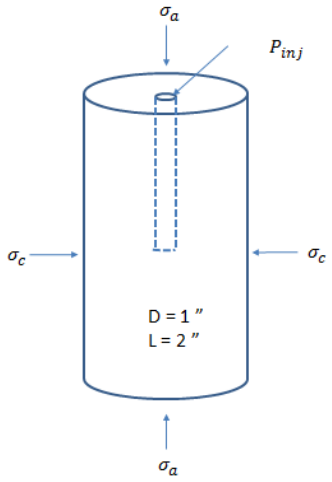

Fig. 3. Sample design.

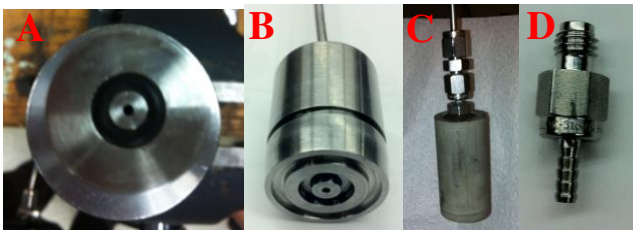

Fig. 4. Sealing methods: A): Single O-ring seal within the platen; B): Double O-ring seal; C): Fitting design; D): Close-up of the fitting with barbs that are epoxied into the blind borehole within the sample.

2.4 Sample Preparation

Green River shale samples are trimmed by saw to a length of 2-inches and then end-ground. A central borehole is machine-shop drilled (~1/10-inch-diameter to depth of 1-inch) to half depth of the sample.

2.5 Standard Test Procedure

The jacketed sample is placed in the apparatus and axial and confining stresses are applied. Once at the desired pressure, the axial stress is held constant and the pump controlling the confining stress set to constant volume with a pressure relaxation ~0.6%. With confining stress set to constant volume, a rapid increase in confining pressure can also be used as a sign for sample failure. Fluid is then injected into the blind borehole at a constant flow rate (1 *ml/min* for H_2O; 5 *ml/min* for CO_2 and N_2). Breakdown in the sample is observed as a rapid drop in the borehole pressure and a simultaneous jump in the confining pressure (Fig. 5). This defines the breakdown pressure with a typical log shown in Fig. 5.

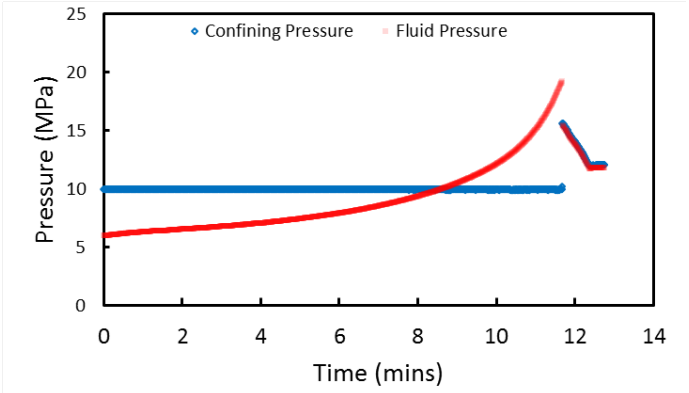

Fig. 5. Typical pressure response during an hydraulic fracturing experiment. (Sample: Green River shale; Stimulant: CO_2; Confining stress: 10 MPa; Axial stress: 20 MPa; Breakdown pressure: 19.3 MPa)

3 RESULTS

Previous studies (Alpern, et al., 2012; Gan, et al., 2013) have shown that the breakdown pressures and morphology of induced fractures are dependent on both the fracturing fluid and the applied stress regime. We explore the mechanistic underpinnings of these observations in the following, together with their consistency with the observed results in this study.

3.1 Theoretical Considerations

Hydraulic fractures initiated from a cylindrical borehole in a simple-triaxial stress regime will open against the minimum principal stress (i.e. in the plane of the maximum principal stress). In our configuration, the fractures should develop either across the borehole (Fig. 6-left) when the axial stress is less than the confining stress, or along the borehole (Fig. 6-right) when the axial stress is the maximum stress.

When the axial stress is the maximum principal stress (Fig. 6-right), failure is based on the Hubbert and Willis (H-W) hydraulic fracturing criterion where the fracture evolves perpendicular to the local minimum principal stress at the borehole wall, when the rock tensile strength is exceeded. If there is no initial pore pressure in the rock, and assuming

an elastic medium, the breakdown pressure is given by:

$$p_b = 3\sigma_{h_{min}} - \sigma_{h_{max}} + \sigma_t \quad (1)$$

where p_b is breakdown pressure, $\sigma_{h_{min}}$ is minimum horizontal stress and $\sigma_{h_{max}}$ is maximum horizontal stress (both perpendicular to the borehole), and σ_t is the tensile strength of the rock.

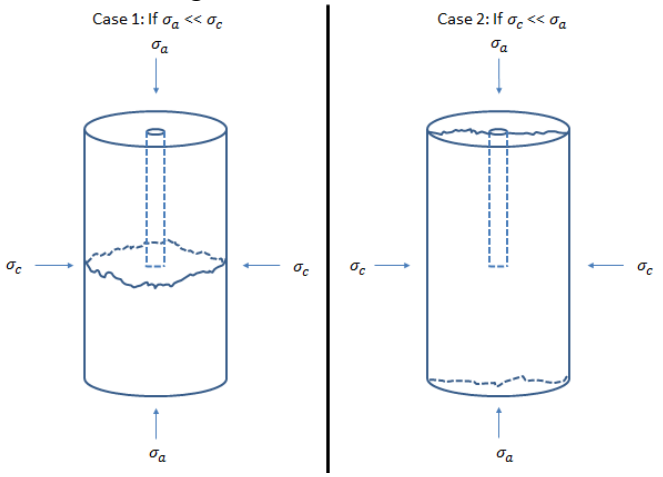

Fig 6. Potential failure modes for different stress configurations.

In our experiments, and for the specific case of the longitudinal fracture of Case 2 then $\sigma_{h\min} = \sigma_{h\max} = \sigma_c$ and the breakdown pressure is given by

$$p_b = 2\sigma_c + \sigma_t \quad (2)$$

where σ_c is the confining pressure ($\sigma_{min} = \sigma_{\max} = \sigma_c$). Thus, for these cylindrical samples, the breakdown pressure should be solely a function of confining pressure for a defined tensile strength.

When the axial stress is the minimum principal stress (Fig. 6-left), the sample fails transversely to the borehole. In this case the stress concentration around the tip of the borehole is undefined at the sharp boundary of the borehole termination – acting as a stress concentrator. Although theoretically undefined and large, it will be limited by blunting of the termination geometry and local failure. In this case the breakdown pressure may be defined generically as

$$p_b = A\sigma_a - B\sigma_C + C\sigma_t \quad (3)$$

where A, B and C are coefficients for axial stress, confining stress and tensile strength. Thus a similar arrangement may be applied to the H-W solution for a longitudinal fracture, with only the magnitudes of the coefficients A and B changing. Absent a stress concentration, the coefficients for Case 1 (when the confining stress is larger) would be $A = C = 1$ and $B = 0$, and for Case 2 (when the axial stress is larger), $A = 0, B = -2, C = 1$.

The results for the above equations are for the case that no fluid penetrates the borehole wall (Hubbert & Willis, 1957). Where fluid penetration occurs, based on poroelastic theory considering the poroelastic stress induced by the fluid permeation into rocks (Haimson & Fairhurst, 1967), the revised expression for both Cases 1 and 2 may be redefined as:

$$p_b = (A'\sigma_a + B'\sigma_c + C'\sigma_t)\frac{1}{1+\eta} \quad (4)$$

$$\eta = \frac{\nu\alpha}{(1-\nu)} \quad (5)$$

where A' is the coefficient for axial stress; B' is the coefficient for confining stress and C' is the coefficient on the tensile strength (always unity); υ is the Poisson ratio and α is the Biot coefficient which reflects the poroelastic effect (Biot, 1941); $\frac{1}{1+\eta}$ ranges between 0.5 (permeable, where fluid is allowed entry into the borehole wall with η=1, α=1 and υ=0.5) and 1 (impermeable, where fluid is excluded from the borehole wall with η=0 and α=0 which results in Eqn. (4) collapsed into Eqn. (3)). Similar to the impermeable cases, when $\sigma_C < \sigma_a$ the coefficients A'=0 and B'=2 for longitudinal fracture (Case 2) ; when $\sigma_C > \sigma_a$ and neglecting the stress concentration effect, A'=1 and B'=0 for transverse fracture (Case 1). In addition, if critical invasion pressure p_c, which is also known as capillary pressure, is known, we can compare it with the breakdown pressure of permeable and impermeable solution to decide if supercritical fluid would indeed have a lower breakdown pressure than subcritical fluid (Fig. 7) (Gan, et al., 2013, 2015).

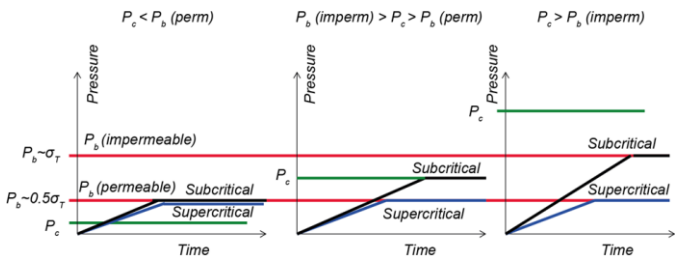

Fig. 7 Critical pressure vs. breakdown pressure under different invasion pressure P_c values (Gan, et al., 2013).

There are three scenarios depending on the critical invasion pressure magnitude:

1. When the invasion pressure is lower than the breakdown pressure in the permeable case, both supercritical and subcritical fluids have the same magnitude of breakdown pressure (Fig. 7-left);
2. When the invasion pressure is intermediate between the breakdown pressure of the permeable and impermeable cases, the subcritical fluid invades and failure occurs at the critical pressure. In this case, supercritical fluids would result in a lower breakdown pressure than the invasion pressure (see Fig. 7-center).
3. When the invasion pressure is larger than the breakdown pressure for both permeable and impermeable cases, the supercritical fluid leads to a lower breakdown pressure than the subcritical fluid (see Fig. 7-right).

3.2 Experimental Results

A large number of experiments are completed on Green River shale under various stress conditions. These experiments are completed for the three fracturing fluids H_2O, CO_2 and N_2.

Results are grouped according to stress conditions and failure modes. For those failing longitudinally where the breakdown pressure is solely a function of confining stress and a given constant tensile strength, breakdown pressures are shown scaled with confining stress (Fig. 8).

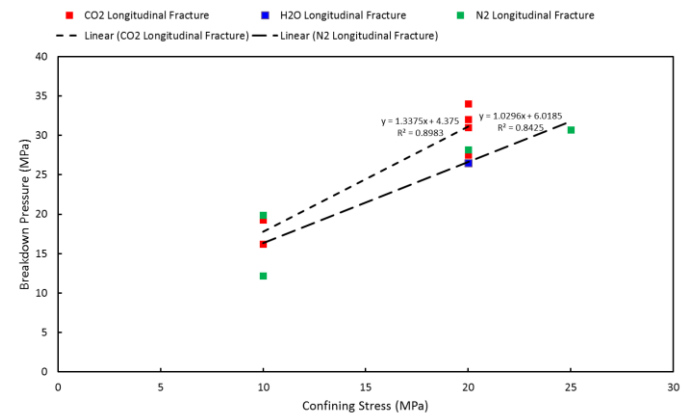

Fig 8. Breakdown pressure as a function of confining stress (Case 2: longitudinal fracture).

Even though the results are somewhat scattered, the general trend is that CO_2 has larger breakdown pressures than N_2, which in turn as higher breakdown pressures than H_2O. If interpreted using the concepts (Eqns. 3-5) discussed previously, the magnitudes of the tensile strength are on the order of 4-6 MPa and the multiplier for the confining stress (B) is ~1-1.3.

When the samples fail in a transverse mode, ignoring the stress concentration effect, the breakdown pressure is principally controlled by axial stress. Breakdown pressures are shown as a function of axial stress in Fig. 9.

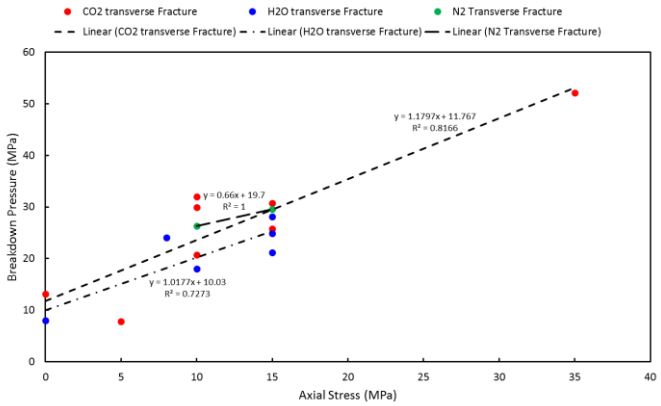

Fig 9. Breakdown pressure as a function of axial stress (Case 1: transverse fracture).

Again, the breakdown pressures are greatest for CO_2, lower for N_2 and lowest for H_2O. Projected tensile strength, is in the order of 12-20 MPa. The coefficient of the axial stress (A) is 0.7-1.2.

3.3 Application to Other Rock Types

Extensive attempts have been made to estimate the magnitude of breakdown pressure through analytical, semi-analytical and numerical approaches (Kutter, 1970; Newman, 1971; Tweed & Rooke, 1973). The suitability of using GRS as an analog for other rock types may be established through comparison of index properties of strength, deformability, porosity and permeability, as well as organic content. These are given in Table 1. More specifically, direct scaling of fracture breakdown is possible when indices of extensional strength (tensile strength) and capillary behavior (scaled from permeability and porosity) are applied.

The Green River shale (GRS) is fine-grained, highly laminated, and with low-grade kerogen. Its geomechanical properties are shown in Table 1.

Table 1. Geomechanical properties of Green River shale.

Rock type	GRS
Tensile strength, σ_T	9.3MPa (load parallel to the bedding) 13.4MPa (load perpendicular to the bedding)
Permeability, k	~10^{-17} m^2 (Culp, 2014)
Porosity, φ	~10% (Morgan, et al., 2002)
	30GPa (Young's modulus) (Aadnoy & Looyeh, 2011)
Bulk Modulus, K	3.5-5GPa (Bulk modulus of Kerogen) (Yan & Han, 2013)
	1.7-2.5GPa (Shear modulus of Kerogen) (Yan & Han, 2013)
Poisson ratio, υ	0.2 (Aadnoy & Looyeh, 2011)
Elastic moduli ratio, n	0.84 (Aadnoy & Looyeh, 2011)
TOC	17%~20%

The various responses for breakdown for GRS in each of the configurations are:

Longitudinal fracture ($\sigma_{\min} = \sigma_c < \sigma_{axial}$):

$$CO_2: \quad p_b = 1.34\,\sigma_{\min} + 4.4\ MPa \tag{6}$$

$$N_2: \quad p_b = 1.04\,\sigma_{\min} + 6.0\ MPa \tag{7}$$

Transverse fracture ($\sigma_{\min} = \sigma_{axial} < \sigma_c$):

$$CO_2: \quad p_b = 1.18\,\sigma_{\min} + 11.8\ MPa \tag{8}$$

$$N_2: \quad p_b = 0.66\,\sigma_{\min} + 19.7\ MPa \tag{9}$$

$$H_2O: \quad p_b = 1.02\,\sigma_{\min} + 10.0\ MPa \tag{10}$$

A straightforward interpretation of these breakdown pressure estimates is that the stress offset is proportional or equal to the tensile strength. Further, the variation of the estimates with different confining or axial stresses are due to the stress regime and the stress concentrations around the borehole. Since the borehole configuration remains the same in all experiments, the results should therefore scale with confining stress and tensile strength.

4. DISCUSSION

A large number of experiments completed in Green River shale indicate the following:

1. Under the same applied stress conditions, CO_2 returns the highest breakdown pressure, followed by N_2, and then H_2O;

2. The distribution in breakdown pressures is of the order of ~25% to ~30% of the maximum breakdown pressure for this progression of fluids from highest (with CO_2) to lowest (with H_2O).

3. Fracturing with CO_2, compared to other fracturing fluids, creates marginally more complex fracturing patterns as well as the coarsest fracture surface and with the greatest apparent local damage (Fig. 10). Image analysis would be required to quantify this (e.g. using the Zygo NexView Optical Profilometer);

Fig. 10: Fracture patterns caused by A): H_2O; B): CO_2; C): N_2. (Sample: Green River shale; Confining stress: 25MPa; Axial stress: 15MPa)

4. Under a constant injection rate, the CO_2 pressure response exhibits a long plateau of constant pressure due to condensation between ~5-7MPa. This condensation period indicates that the CO_2 transits from gas to liquid through a mixed-phase region. Due to the nature of the other gases, this is not observed for H_2O and N_2.(Fig. 11);

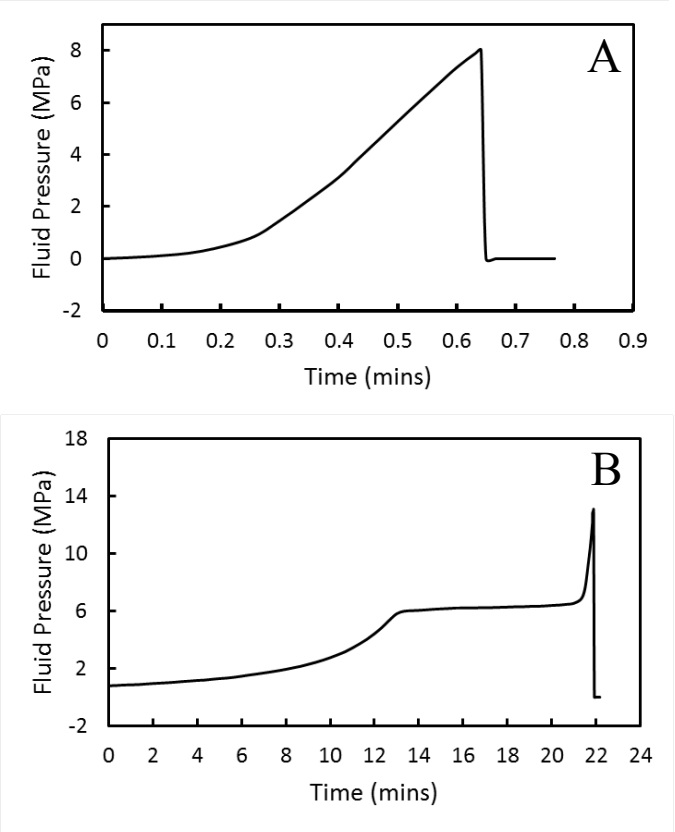

Fig. 11: Typical fluid pressure profiles for fracturing with A) H_2O and B) CO_2, which shows gas condensation behavior between ~5-7 MPa.

5. There is a positive correlation between minimum principal stress and breakdown pressure for failure in both transverse fracturing ($_3$ *axial*) and longitudinal fracturing ($_3$ *radial*). CO_2 has the highest correlation coefficient/slope and H_2O has the lowest. This observation can be explained with the specific properties of the stimulating fluids.

Reference

1. Morgan, C. D. et al., 2002. *Characterization of Oil Reservoirs in the Lower and Middle Members of the Green River Formation, Southwest Uinta Basin, Utah*. Wyoming, AAPG Rocky Mountain Section Meeting AAPG Rocky Mountain Section Meeting.
2. Aadnoy, B. & Looyeh, R., 2011. *Petroleum Rock Mechanics: Drilling Operations and Well Design*. June 9, 2011 ed. s.l.:Gulf Professional Publishing.
3. Alpern, J. et al., 2012. Exploring the physicochemical processes that govern hydraulic fracture through laboratory experiments. *46th US Symposium on Rock Mechanics and Geomechanics*.
4. Biot, M. A., 1941. General theory of three-dimensional consolidation. *Journal of Applied Physics*, 12(2), pp. 155-164.
5. Bullis, K., 2013. *Skipping the Water in Fracking-The push to extend fracking to arid regions is drawing attention to water-free techniques*. [Online] Available at: http://www.technologyreview.com/news/512656/skipping-the-water-in-fracking/ [Accessed 22nd Feb. 2015].
6. Culp, B., 2014. Impact of CO2 On Fracture Complexity When Used As A Fracture Fluid In Rock. *A Thesis in Geoscience*.
7. Faraj, B. & Brown, M., 2010. *Key Attributes of Canadian and U.S. Productive Shales: Scale and Variability*. New Orleans, AAPG Annual Convention.
8. Friehauf, K. E., 2009. Simulation and design of energized hydraulic fractures. *UT Austion Doctor of Philosophy Dissertation*.
9. Friehauf, K. E. & Sharma, M. M., 2009. *Fluid Selection for Energized Hydraulic Fractures*. New Orleans, SPE Annual Technical Conference and Exhibition.
10. Gan, Q. et al., 2013. Breakdown pressures due to infiltration and exclusion in finite length boreholes. *47th US Symposium on Rock Mechanics and Geomechanics*.
11. Gupta, S. D. et al., 2009. Development and Field Application of a Low pH, Efficient Fracturing Fluid for Tight Gas Fields in the Greater Green River Basin, Wyoming. *SPE Production & Operations*, 24(04), pp. 602-610.
12. Haimson, B. & Fairhurst, C., 1967. Initiation and extension of hydraulic fractures in rocks. *SPE*, pp. 310-318.
13. Hall, R., Chen, Y., Pope, T. L. & Lee, J. C., 2005. *Novel CO2-Emulsified Viscoelastic Surfactant Fracturing Fluid System*. Dallas, SPE Annual Technical Conference and Exhibition.
14. Hubbert, M. K. & Willis, D. G., 1957. Mechanics of hydraulic fracturing. *Transactions of Society of Petroleum Engineers of AIME*, Volume 210, pp. 153-168.
15. Ishida, T. et al., 2012. Acoustic emission monitoring of hydraulic fracturing laboratory experiment with supercritical and liquid CO2. *Geophysical Research Letters*, 39(16).
16. King, G. E., 2010. *Thirty Years of Gas Shale Fracturing: What Have We Learned?*. Florence, SPE Annual Technical Conference and Exhibition.
17. Kutter, H. K., 1970. Stress analysis of a pressurized circular hole with radial cracks in an infinite elastic plate. *Int. J. Fracture*, Volume 6, pp. 233-247.
18. Newman, J. C., 1971. An improved method of collocation for the stress analysis of cracked plates with various shaped boundaries. *NASA TN*, pp. 1-45.
19. Ribeiro, L. & Sharma, M., 2013. *Fluid Selection for Energized Fracture Treatments*. The Woodlands, SPE Hydraulic Fracturing Technology Conference.
20. Tweed, J. & Rooke, D. P., 1973. The distribution of stress near the tip of a radical crack at the edge of a circular hole. *Int. J. Engng. Sci.*, Volume 11, pp. 1185-1195.
21. Vincent , M. C., 2010. *Refracs: Why Do They Work, and Why Do They Fail in 100 Published Field Studies?*. Florence, SPE Annual Technical Conference and Exhibition.

22. Wang, S., Elsworth, D. & Liu, J., 2011. Permeability evolution in fractured coal: The roles of fracture geometry and water-content. *International Journal of Coal Geology*, pp. 13-25.
23. Yan, F. & Han, D.-h., 2013. *Measurement of elastic properties of kerogen*. Houston, SEG Houston 2013 Annual Meeting .